Am J Nucl Med Mol Imaging 2017;7(3):92-104
www.ajnmmi.us /ISSN:2160-8407/ajnmmi0056575

Original Article

Value of ^{99m}Tc-MDP SPECT/CT and ^{18}F-FDG PET/CT scanning in the evaluation of malignantly transformed fibrous dysplasia

Wei-Jun Wei[1,2*], Zhen-Kui Sun[1*], Chen-Tian Shen[1], Xin-Yun Zhang[1], Juan Tang[3], Hong-Jun Song[1], Zhong-Ling Qiu[1], Quan-Yong Luo[1]

Departments of [1]Nuclear Medicine, [3]Pathology, Shanghai Jiao Tong University Affiliated Sixth People's Hospital, 600# Yishan Road, 200233, Shanghai, China; [2]Shanghai Jiao Tong University School of Medicine, China. [*]Equal contributors and co-first authors.

Received May 2, 2017; Accepted May 10, 2017; Epub July 15, 2017; Published July 30, 2017

Abstract: Although fibrous dysplasia is not considered a potentially premalignant disorder, malignant transformation occurs. Because of its rarity, radiographic features of malignantly transformed fibrous dysplasia on cross-sectional imaging modalities are less recognized, making diagnosis and differential diagnosis of the disease quite difficult in clinical practice. In this study, we analyzed the clinical characteristics, imaging features, pathology findings and surgery strategies of 19 malignantly transformed fibrous dysplasia. We found that there was significant male predominance in this specific cohort (13/6). While osteosarcoma (63.2%) was the most frequently occurring neoplasm secondary to fibrous dysplasia, other less commonly malignantly changed types included fasciculated sarcoma, malignant fibrous histiocytoma, fibrosarcoma and chondrosarcoma. We found that the diagnostic value of single modality imaging method, like conventional X-ray, computed tomography or non-contrast magnetic resonance imaging, was limited mainly because of a lack of whole-body metabolic information. In contrast, we highlighted that ^{99m}Tc-MDP SPECT/CT and/or ^{18}F-FDG PET/CT scanning could exert a pivotal role in the management of malignantly transformed fibrous dysplasia by guiding precise biopsy and optimizing surgery options.

Keywords: Fibrous dysplasia, malignant transformation, osteosarcoma, fibrosarcoma, nuclear medicine imaging

Introduction

Fibrous dysplasia (FD) is a benign disorder of the bone, with monostotic fibrous dysplasia significantly more common than polyostotic disease. Monostotic fibrous dysplasia is frequently encountered in adolescents and young adults and usually becomes inactive at the onset of puberty. Because of its nonspecific symptoms including pain, swelling, and pathologic fracture, monostotic fibrous dysplasia is often diagnosed incidentally on radiographic examinations. Polyostotic fibrous dysplasia represents approximately 20-30% of all cases and can frequently involve the pelvis (78%), femur (92%), tibia (82%), craniofacial bones (~50%), upper extremities, ribs, shoulder girdle and spine [1]. Polyostotic variants can be further classified into monomelic and polymelic subtypes. While the former affects the lower extremities and ipsilateral hemi-pelvis, the latter usually involves the extremities, axial skeleton, and craniofacial bones. It has been reported that polyostotic fibrous dysplasia typically presents during the first decade, and the relatively earlier age distribution is related to more severe clinical symptoms.

Although rare, malignant transformation of fibrous dysplasia occurs in up to 2.5% of all cases [2]. Clinically, these patients may present with increasing pain, swelling and/or pathological/stress fracture. Radiologically, a fibrous dysplasia-like lesion with radiographic features of cortical destruction generally suggests low-grade central osteosarcoma or malignant transformation [2]. Other radiographic changes may include osteolysis and adjacent soft-tissue mass. However, the radiographic features of malignantly transformed FD on cross-sectional

Table 1. Clinical and pathological characteristics of the included patients

No (#).	Sex	Subtype	Age	Symptoms	Site	Treatment	Imaging Modalities	Pathology
1	F	Mono-FD	52	Swelling, pain, LOM[1]	Femur	Tumor resection, prosthetic replacement	X-ray, CT, MRI	Osteosarcoma
2	M	Mono-FD	54	Pathological fracture of femur	Femur	Tumor resection, prosthetic replacement, amputation, chemotherapy	X-ray, MRI, ^{99m}Tc-MDP bone scan, PET/CT	Osteosarcoma
3	F	Mono-FD	45	Swelling, pain	Tibia	Curettage , bone graft & fixation	X-ray, ^{99m}Tc-MDP bone scan	Osteosarcoma
4	F	Mono-FD	20	Swelling, pain, LOM	Tibia	Tumor resection, total knee replacement	X-ray, CT, Untrasound	Fasciculated sarcoma
5	M	Poly- FD	48	Tenderness	Femur, tibia, ilium, pubis	Bone graft & fixation , tumor resection, total knee replacement, chemotherapy	X-ray, CT, MRI, ^{99m}Tc-MDP bone scan, PET/CT	Osteosarcoma
6	F	Mono-FD	46	Tenderness, swelling	Femur	Curettage, bone graft & fixation, tumor resection, prosthetic replacement, chemotherapy	X-ray, CT, MRI, PET/CT	Osteosarcoma
7	M	Mono-FD	25	Swelling	Femur	Tumor resection, prosthetic replacement	X-ray, CT, MRI	MFH[2]
8	M	Mono-FD	14	Pathological fracture	Humerus	Free fibula transplantation and fixation	X-ray	Fibrosarcoma
9	M	Mono-FD	47	Pathological fracture	Femur	Curettage, chemotherapy, amputation	X-ray, MRI	Osteosarcoma
10	M	Mono-FD	68	Pain, LOM	Tibia	Tumor resection, prosthetic replacement, amputation	X-ray ,CT guided biopsy	Fasciculated sarcoma
11	F	Poly-FD	33	Swelling, pain, LOM	Humerus, shoulder blade, ribs, femur, ilium	Tumor resection, prosthetic replacement, chemotherapy, zoledronic acid	X-ray, CT, MRI, PET/CT	Osteosarcoma, ABC[3]
12	M	Poly-FD	44	Blindness, numbness	Skull, ribs, vertebrae	Resection of pituitary tumor, Chemotherapy	CT guided biopsy, X-ray, CT, MRI, ^{99m}Tc-MDP bone scan	Osteosarcoma, chondrosarcoma
13	M	Poly-FD	35	Pathological fracture	Femur, ilium, Humerus	Curettage, autologous Ilium graft, amputation, chemotherapy	CT, MRI, PET/CT	Osteosarcoma, fibrosarcoma
14	M	Mono-FD	36	Swelling, pain, malunion	Radial bone	Tumor resection, free fibula transplantation and fixation, ulna rection & joint fusion	X-ray, CT, MRI	Osteosarcoma
15	M	Poly-FD	86	Swelling, pain, LOM	Radial bone, Humerus	Amputation	X-ray, CT, CT guided biopsy, ^{99m}Tc-MDP bone scan, PET/CT	Osteosarcoma
16	M	Mono-FD	14	Routine examination	Femur	Curettage, bone graft & fixation	X-ray, CT, MRI, CT guided biopsy	Undetermined
17	M	Mono-FD	45	Swelling, pain, LOM	Tibia	Curettage, bone graft & fixation, amputation	X-ray, CT,	Fasciculated sarcoma
18	F	Mono-FD	23	Swelling, pain, LOM	Femur	Amputation, Chemotherapy	X-ray, CT, MRI, CT guided biopsy	Osteosarcoma
19	M	Poly-FD	43	Swelling, pain	Femur, tibia	Amputation, Chemotherapy	X-ray, CT, MRI, ^{99m}Tc-MDP bone scan	MFH[2]

[1]LOM, limitation of motion; [2]MFH, malignant fibrous histiocytoma; [3]ABC, aneurysmal bone cyst.

imaging modalities and their post-therapeutic radiological features are less recognized. Here, we summarized the clinicopathologic and radiologic features of 19 malignantly transformed FD cases. More importantly, we highlighted that nuclear medicine imaging modalities, ^{99m}Tc-MDP SPECT/CT and ^{18}F-FDG PET/CT could play a pivotal role in assessing malignant transformation of FD, in detecting disease recurrence and in optimizing the biopsy site.

Methods, patients and imaging modalities

This retrospective study was approved by our institutional review board. Pathology, radiology and electronic health record (EHR) systems were indexed when screening potential candidates for this study. The inclusion criteria were as follows: (1) patients with initial histologically proven FD; (2) patients who received at least one modality radiological examination; (3) the FD underwent malignant transformation discovered upon follow-up and was confirmed by histopathology; and (4) patients had integral EHRs, especially operation records and other non-operative treatment recordings such as chemotherapy records. Informed consent was waived for most patients except for those whose images were used in the current study. All methods were performed in accordance with the relevant guidelines and regulations.

For ^{18}F-FDG PET/CT scans, the patients were instructed to fast for at least 6 hours before the injection of ^{18}F-FDG. The blood glucose level was measured before injection, and ^{18}F-FDG was administered at glucose levels <150 mg/dL. ^{18}F-PET/CT scanning was performed one hour after i.v. injection of 3-4 MBq/Kg ^{18}F-FDG. Generally, no intravenous contrast agent was administered. ^{18}F-FDG PET/CT images were performed using a dedicated GE Discovery PET/CT scanner including 64-slice CT scanners with a dedicated PET (BGO plus crystal). ^{18}F-FDG images were acquired for 4 minutes at each bed position from the skull base to the superior mediastinum with the patients' arms along the chest and from the neck to the mid-thigh with the patients' arms above the head. No specific breathing instructions were given. CT scanning was obtained from the orbitomeatal line (OML) and progressed to the mid-thigh using a standardized protocol involving 140 kV, 110 mA, 0.8 seconds/rotation, a pitch of 1.75:1, a length of scan of 1.0 to 1.6 m and a slice thickness of 3.75 mm. Attenuation correction of PET images was performed using attenuation data from CT, and image reconstruction was performed using a standard reconstruction algorithm with ordered subset expectation maximization (OSEM). Image fusion was performed using coordinate-based fusion software and was subsequently reviewed at a workstation (Xeleris) that provided multi-planar reformatted images and displayed PET, CT, and PET/CT fusion images. ^{99m}Tc-MDP SPECT/CT, CT and MRI imaging were acquired according to our previously reported instructions [3, 4].

Results

Clinical and pathological characteristics

Of 19 malignantly transformed FDs, 13 (68.4%) were of the monostotic subtype with an average patient age of 37.6±17.0 yrs, and the remaining 6 (31.6%) were of the polyostotic subtype with an average patient age of 40.95±18.0 yrs. There was significant male predominance in this cohort (13/6). While pain, swelling, and limitation of motion (LOM) were the most common clinical symptoms and signs, 4 patients were initially admitted to the hospital for the evaluation of pathological fracture (#2, #8, #9, #13; **Table 1**). One patient (#12, 5.6%) with polyostotic lesions developed McCune-Albright syndrome (MAS) associated with a pituitary tumor but without café-au-lait pigmentation of the skin. Craniofacial lesions of the patient resulted in the impingement of cranial nerves-the optic nerve and auditory nerve-affection of middle ear structures, and deformity. Of the included patients, monostotic and polyostotic forms arose more frequently in the long bones (proximal femur, tibia and humerus) and less frequently in the craniofacial bones (maxilla and mandible), ribs, ilium, pubis, radial bone, vertebrae and shoulder blade. All monostotic diseases affected a single bone with one focus. Of the 6 poly-type patients, while 3 cases presenting with polyostotic monomelic FD involved the homolateral lower limb and ilium (#5, #19) and humerus and radial bone (#15), the remaining 3 patients showed more severe polymelic FD (#11, #12, #13). Although the spine was an infrequent location, 1 patient (#12) showed spine involvement associated with the polyostotic form. Histopathology revealed that osteosarcoma (63.2%) was the most frequently occurring neoplasm, followed by fasciculated

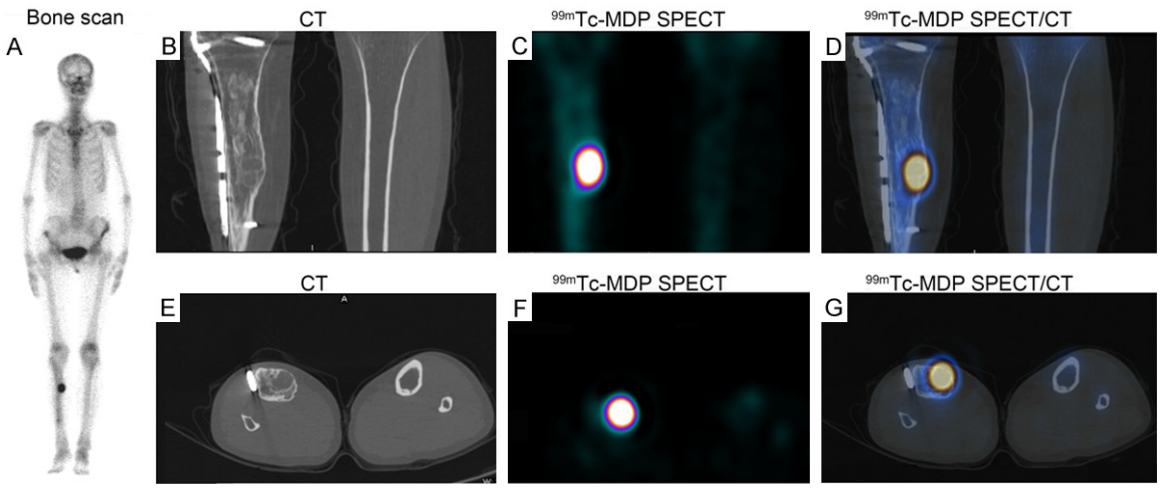

Figure 1. Malignant transformation of fibrous dysplasia to osteosarcoma in a 45-year-old woman presenting with swelling and pain. ^{99m}Tc-MDP bone scan and SPECT/CT fusion images of the patient disclosed a positive finding. A: Delayed scintigram showed focal radionuclide activity. B-D: Reformatted coronal non-contrast CT of the proximal tibia showed an oval low-density area accompanied by increased uptake of radiotracer. E-G: Corresponding axial fusion images confirmed the above findings.

sarcoma (15.8%), malignant fibrous histiocytoma (10.5%), fibrosarcoma (10.5%), chondrosarcoma and undetermined pathology type. It was notable that the pathology results of two patients revealed mixed malignant components (#12, #13) (**Table 1**).

Diagnostic modalities

For fibrous dysplasia, radiographs depict a well-circumscribed lucent lesion in the metaphysis or diaphysis with a ground-glass appearance. The cortical bone may be thinned with diffuse endosteal scalloping. Periosteal reaction is usually not seen unless a pathologic fracture appears [5]. Compared with radiographs, CT is a better technique for characterizing the sclerotic margin of the lesion and visualizing the cortical detail. Fibrous dysplasia enhances with the administration of intravenous contrast material due to the inherent vascularity of the lesion. The MR imaging appearance may not be helpful in differentiating fibrous dysplasia from other bone lesions [6]. Nuclear medicine imaging modalities may be more effective tools for identifying the size of the area affected by malignantly transformed FD and could be useful when the radiographic appearance of suspected canceration is ambiguous [7]. Actually, 9 of 19 patients received ^{99m}Tc-MDP SPECT/CT and/or ^{18}F-FDG PET/CT examinations in the cohort reported here (**Table 1**), eventually facilitating a more precise biopsy and a more optimal surgery strategy. The imaging features of the included patients were assessed from the following aspects: margins, periosteal reaction, multiplicity of lesions, soft-tissue involvement, enhancement and metabolic changes.

Imaging features and typical cases

Long bone FD demonstrates the classic features of fibrous dysplasia: intramedullary, predominantly diaphyseal, ground-glass density; expansive, well-defined often sclerotic borders (rind); endosteal erosions; intact cortex; and variable bone remodeling. Of the 10 long-bone FD cases that underwent osteosarcoma canceration, 7 patients received ^{99m}Tc-MDP bone scans and/or ^{18}F-FDG PET/CT examinations. Patient 3 (#3) received treatment for FD in the right tibia with curettage and bone grafting on 10/2012. Histopathology disclosed that part of the disease had characteristics of intraosseous well-differentiated osteosarcoma that had penetrated the adjacent cortical plate and infiltrated parosteal soft tissue. Postoperative anteroposterior and lateral radiographs of the patient are shown (Supplementary Figure 1A, 1B). Four years later, the patient complained of recurrent bone pain, but routine X-ray examinations reported no significant findings (Supplementary Figure 1C, 1D). However, further ^{99m}Tc-MDP SPECT/CT examination showed intense focal uptake of the radiotracer in the proximal end of the right tibia accompanied by expansile

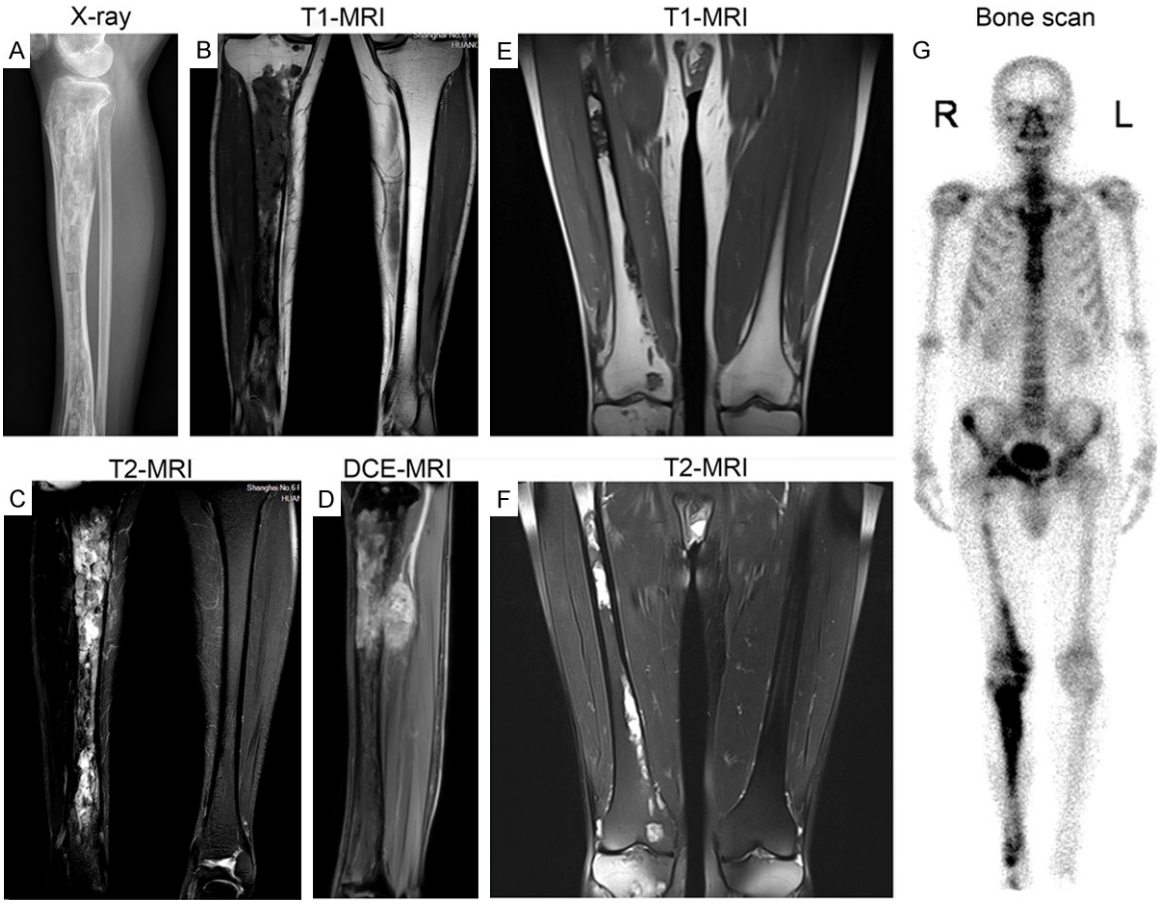

Figure 2. Malignant transformation of fibrous dysplasia to osteosarcoma in a 48-year-old man presenting with tenderness (patient 5). A: Lateral X-ray examination after initial bone grafting and fixation surgery. B, C: T1- and T2-weighted MRI showed heterogeneous signal intensity of the involved right tibia but no obvious remnant or recurrent disease. D: Sagittal dynamic contrast-enhanced MRI (DCE-MRI) showed a well-circumscribed soft-tissue mass enhanced significantly after injection of MRI contrast agent. E, F: T1- and T2-weighted MRI of bilateral femoral bones showed that the right tibia of the patient was also infiltrated by FD. G: ^{99m}Tc-MDP bone scan showed sites of polyostotic FD with dense uptake, indicating monomelic subtype of Poly-FD in this patient.

well-circumscribed lesions on corresponding CT images, indicating remnant or, more likely, recurrence of the disease (**Figure 1**). Patient 5 (#5) initially came to the hospital complaining of right tibia pain in 07/2013, and initial radiological examinations revealed FD. The patient then received curettage, bone grafting and fixation surgery (**Figure 2A**). Upon follow-up (08/2015), coronal T1-weighted imaging (T1 WI) showed that the lesion together with the packing materials was isointense to muscle (**Figure 2B**). Coronal STIR MR imaging showed that the lesions were hyperintense to muscle and seemingly invaded adjacent cortical bone (**Figure 2C**), and dynamic contrast enhanced MRI (DCE-MRI) showed that one lesion was enhanced significantly (**Figure 2D**). Notably, we also found that the right femur of the patient was involved concomitantly (**Figure 2E**, **2F**). In the presence of the massive prosthesis, the bone scan of the patient showed uptake of radiotracer in the distal right femur and proximal right tibia, possibly representing remnant and/or recurrent disease (**Figure 2G**). In the context of prosthesis, the bone scan can also be helpful in demonstrating complications, such as loosening or infection [8]. ^{18}F-FDG PET/CT can be extremely helpful in locating sites of disease where the anatomy is complex or altered by surgery. It may locate disease when other cross-sectional imaging modalities have demonstrated normal size nodes [9]. Despite diffuse diseased areas on MRI and bone scan images (**Figure 2**), subsequent ^{18}F-FDG PET/CT examination demonstrated intense

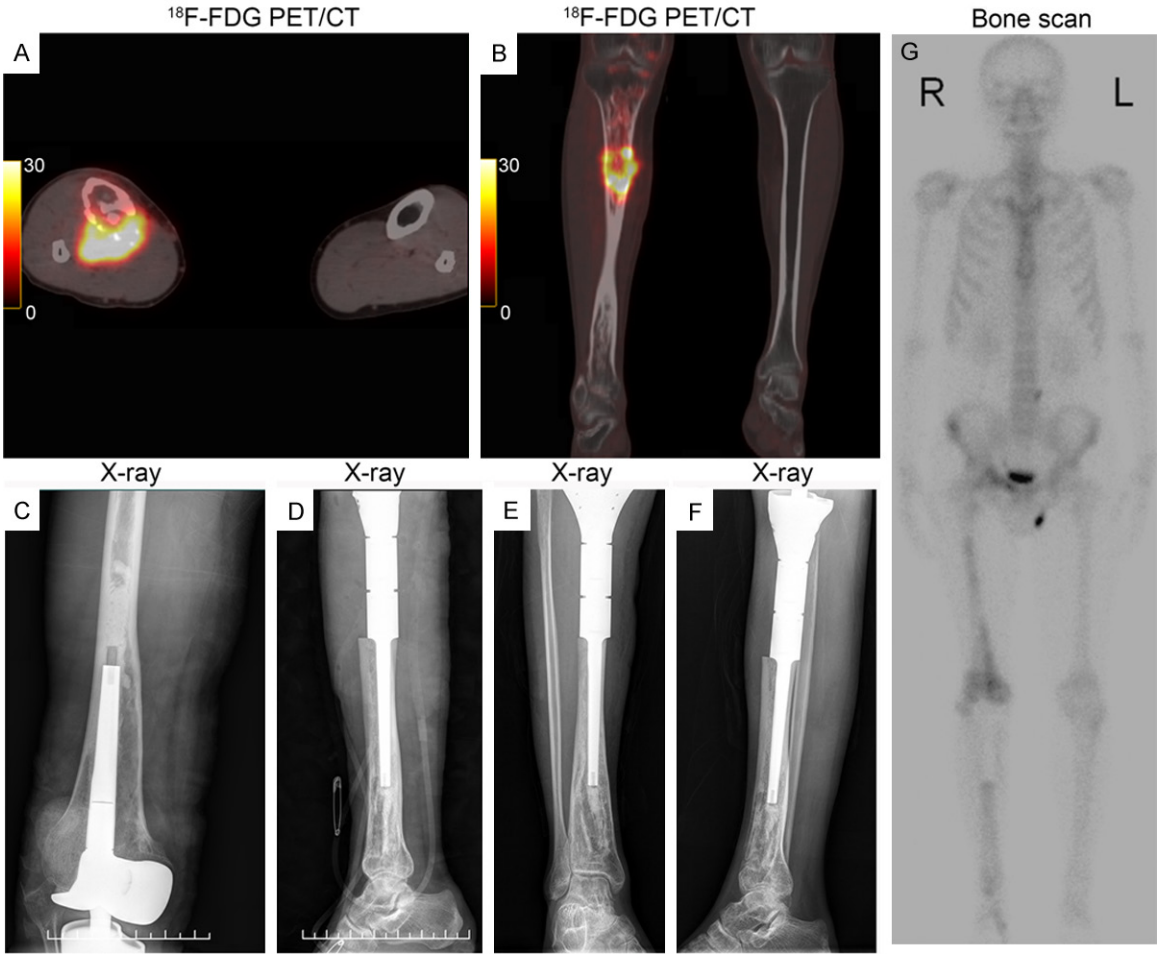

Figure 3. Preoperative and postoperative medical imaging examinations of patient 5. A, B: Axial and coronal PET/CT fusion images demonstrated recurrence of the tumor with increased ^{18}F-FDG uptake with SUV_{max} of 23. C, D: Anteroposterior and lateral radiographs performed after the second surgery. E, F: Anteroposterior and lateral radiographs performed two months after second the surgery. G: ^{99m}Tc-MDP bone scan performed 7 months after the second surgery showed successful resection of the tumor tissue without notable disease remnants or recurrence.

focal uptake of the radiotracer in the proximal right tibia (SUV_{max}=23, **Figure 3A**, **3B**). The combination of PET/CT scanning with conventional imaging changed the management of the patient from extensive high amputation to more conserved tumor resection and total knee replacement (**Figure 3C-F**). Bone scan performed 7 months after the second surgery showed postoperative imaging without notable disease remnants (03/2016, **Figure 3G**). The additional value of ^{18}F-FDG PET/CT in detecting osteosarcoma recurrence secondary to FD canceration was further consolidated by patient 6 (Supplementary Figure 2). However, the differential diagnosis of osteosarcoma recurrence from postoperative myositis ossificans, a rare benign cause of heterotopic bone formation within soft tissue, is sometimes challenging because the latter may also show ^{18}F-FDG uptake [10-12].

Primary osteosarcoma most frequently affects long bones, particularly around the knee joints. However, it seemed that this rule did not apply to the secondary osteosarcomas reported here because 4 (#11, #12, #14, #15) of the included secondary osteosarcomas arose from generally less involved bones (**Table 1**). A typical case was patient 15, who was an 86-year-old male patient admitted to our hospital for the evaluation of swelling and tenderness of the right forearm. Initial X-ray, CT and MRI imaging indicated possible FD in the middle segment of the right radius. However, ^{18}F-FDG PET/CT scanning revealed pathological fracture together

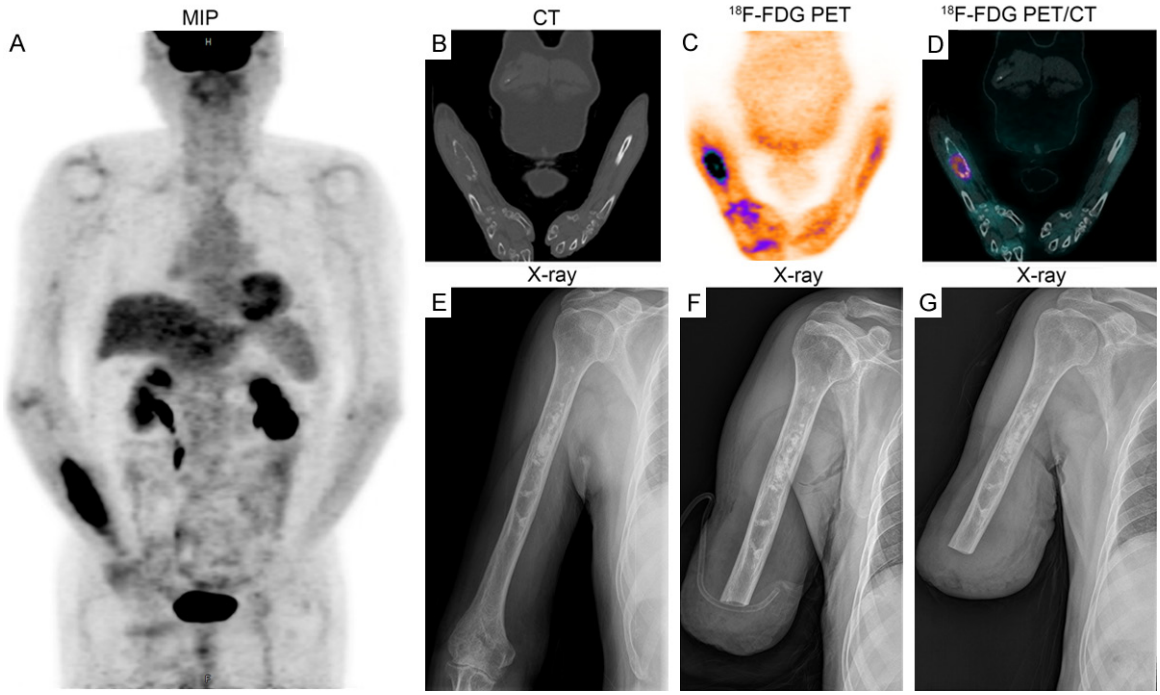

Figure 4. Malignant transformation of fibrous dysplasia to osteosarcoma in an 86-year-old male presenting with swelling, pain, and limitation of motion (Patient 15). A: Maximum intensity projection (MIP) of the patient revealed increased uptake of radionuclide in the right forearm. B-D: Fusion ^{18}F-FDG PET/CT images revealed discontinuity of cortex of the right radius accompanied by increased glucose metabolism. E: The radiograph further showed multiple enchondroma-like lesions in the diaphysis of the right humerus. F, G: Radiographs taken five days and one month after amputation revealed stable diseases in the diaphysis of the right humerus.

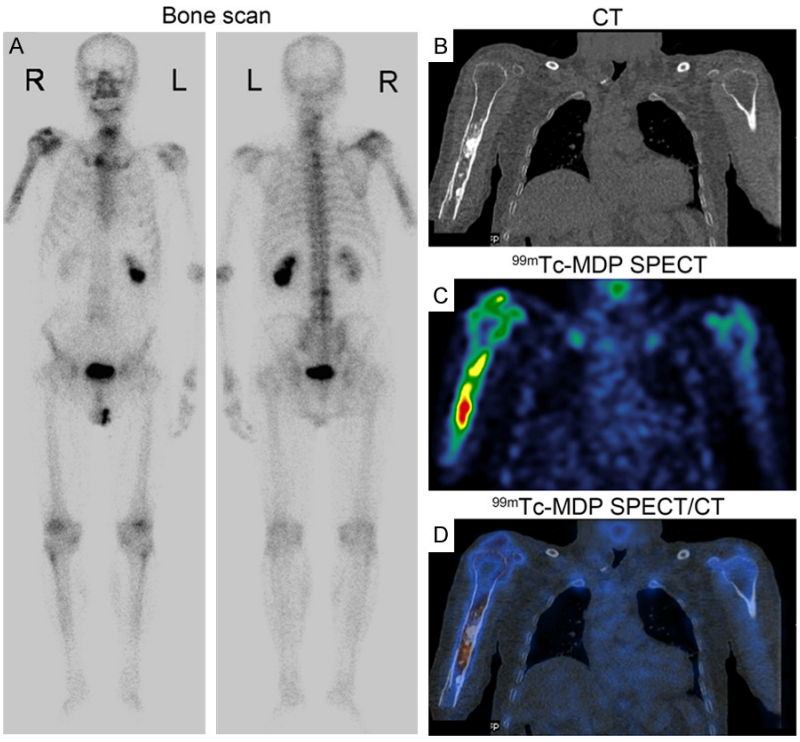

Figure 5. ^{99m}Tc-MDP bone scan and corresponding SPECT/CT fusion images taken half a year after surgery. A: The delayed bone scan showed abnormal ^{99m}Tc-MDP uptake in the upper end of the right humerus. B-D: SPECT/CT fusion images confirmed that the increased concentration of radiotracer coincided with enchondroma-like lesions in the diaphysis.

with intense radiotracer uptake with SUV_{max} of 7.6 in the corresponding area (05/2016, **Figure 4A-D**). Additional multiple calcifications in the medullary cavity of the right humerus were also noted. X-ray confirmed multiple dense, spotty calcifications in the medullary cavity of the right humerus without bony destruction or soft tissue involvement (**Figure 4E**). The patient then received conservative amputation surgery, and postoperative histopathology confirmed

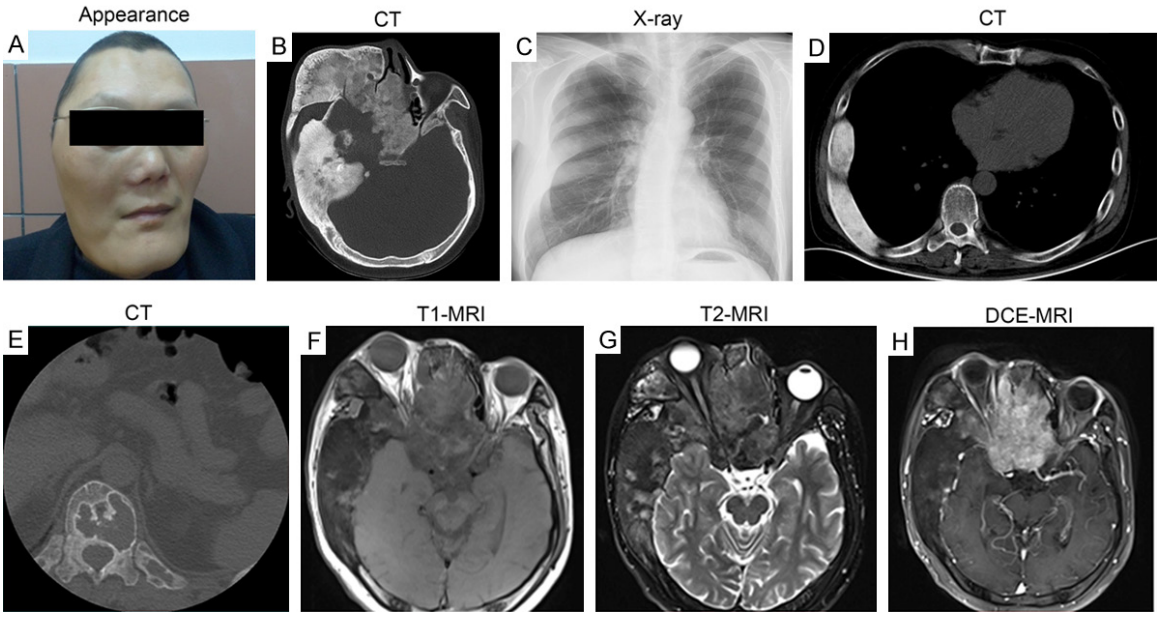

Figure 6. McCune-Albright syndrome of in a 44-year-old male patient with polyostotic fibrous dysplasia (Patient 12). A: Facial deformity of the patient. B: Coronal reformatted CT image demonstrated craniofacial fibrous dysplasia with a ground glass matrix, expansion of the diploic space, and deformity of the involved bones. There was cortical sparing, unlike the cortical thickening of Paget's disease. C, D: Anteroposterior chest radiograph and chest CT showed thickening, osseous expansion, and deformity of the patient's ribs. E: Axial CT of the lower thoracic spine showed expansive, radiolucent lesions of the vertebral body, adjacent ribs and appendix of vertebra. F, G: Brain T1 and T2 weighted MR imaging showed expansion of the medullary canal of the right temporal bone and compression of the patient's cranial cavity. Involvement of the nasal cavity by the poly-FD tissue was also observed. H: Poly-FD tissue in the nasal cavity enhanced significantly after the administration of contrast agent.

the malignant transformation of FD and that the major component of the examined tissue was osteosarcoma. Follow-up ^{99m}Tc-MDP SPECT/CT revealed that enchondroma-like lesions in the right humerus concentrated MDP accompanied by the abnormal uptake of the radiotracer in the left kidney, indicating nephrydrosis (12/2016, **Figure 5**). Enchondroma is a common benign intramedullary neoplasm composed of mature hyaline cartilage, which is most frequently found in the small tubular bones of the hands and less frequently in the proximal humerus and proximal and distal femur and tibia [13]. Multiple enchondromatosis consists of Ollier's disease and Maffucci's syndrome. The former is a rare condition in which multiple enchondromas are present, frequently leading to significant deformity. The latter often presents with multiple enchondromas and multiple soft tissue hemangiomas. Both Ollier's disease and Maffucci's disease are much more prone to the development of secondary chondrosarcoma than patients with a solitary enchondroma [14-16]. Regarding this patient, we tend to believe that diseases in the right radial bone and humerus are of the same origin, although they have different imaging features.

As mentioned above, craniofacial bones (especially the mandible and maxilla), ribs, and femurs are the most commonly affected sites by poly-FD. Skull base lesions of patient 12 involved the greater and lesser wings of the sphenoid bone and further extended into the facial bones. These lesions were expansile and demonstrated increased sclerosis. The above observations were associated with the obliteration of the right frontal/sphenoid/maxillary sinuses, displacement of the right posterior orbital and auditory canals (**Figure 6A**, **6B**). Deformed ribs (**Figure 6C**, **6D**) and expansive spinal lesions with septations were also observed (**Figure 6E**). MR imaging was taken to assess the involvement of the brain tissue. Brain MRI showed heterogeneous high signal intensity on T2 WI, notably, disease in the nasal septum enhanced significantly after injection of the gadolinium contrast agent (**Figure 6F-H**). CT-guided biopsy in the pterygomaxillary fossa

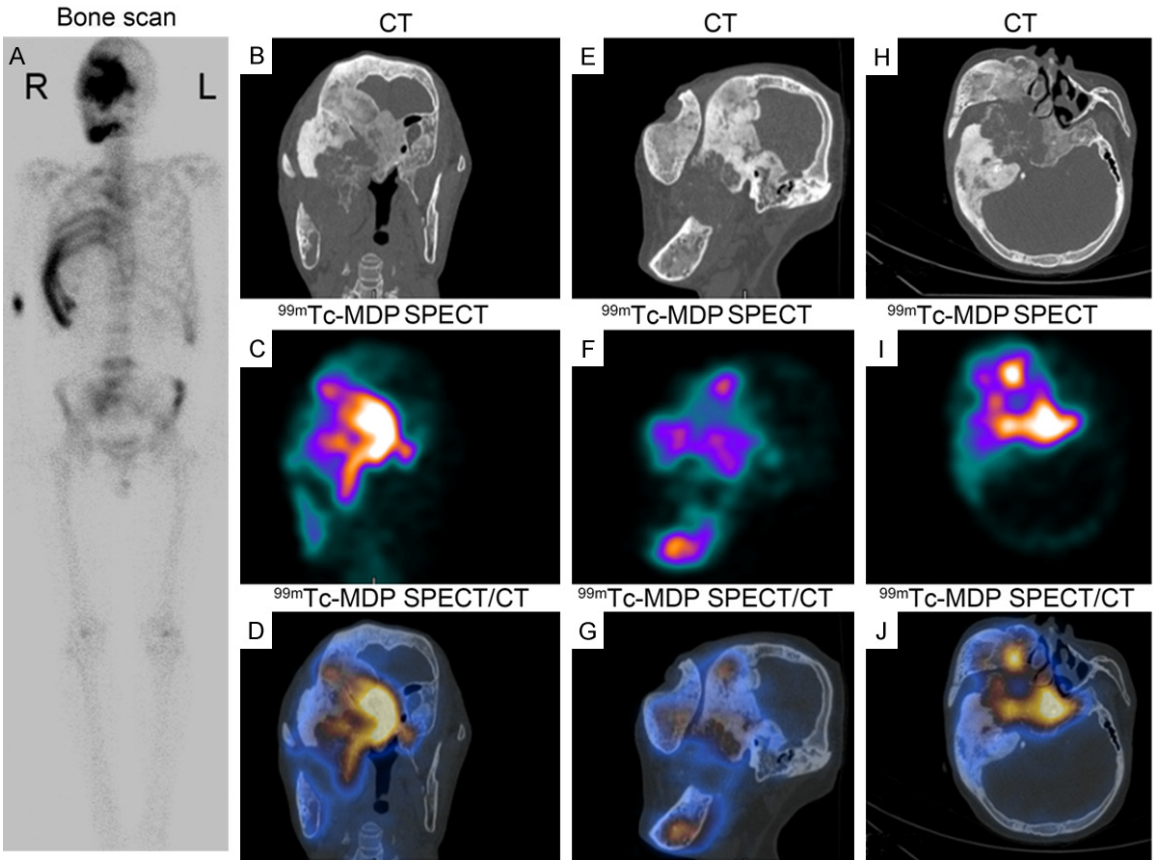

Figure 7. A: ^{99m}Tc-MDP bone scintigraphy helped depict the extent and distribution of the polyostotic FD. Note the lesions in the skull, submaxilla, ribs, pelvis, and vertebrae. B-J: SPECT/CT fusion images demonstrated a ground glass matrix on CT images and increased radiotracer uptake in the corresponding SPECT and fusion images.

revealed that malignantly transformed tissue contained not only osteosarcoma but also chondrosarcoma. Clinically, the patient showed vision deterioration of the right eye and hearing impairment of the right ear. The patient received cycles of chemotherapy but responded minimally as assessed by post-therapeutic SPECT/CT scanning and MRI imaging (**Figure 7** and data not shown). The medical imaging findings of the patient were similar to those of previously reported poly-FD [5]. Only one polyostotic FD patient (5.3%) in our cohort developed McCune-Albright syndrome (MAS), a finding that was consistent with that in a previous study reporting one case with polyostotic disease and sarcoma (3.6%) [2].

Two of our patients (#8, #13) underwent fibrosarcoma transformation, which has no known causes and may appear secondarily on numerous conditions like fibrous dysplasia, Paget's disease, Ollier's disease, osteochondromatosis, giant cell tumor, bone infarct, dedifferentiated chondrosarcoma and dedifferentiated parosteal osteosarcoma. Similar to osteosarcoma, fibrosarcoma had a preference for metaphyses of the long bones, especially the distal femur (#13), followed by the proximal femur, distal humerus (#8), proximal tibia, and pelvis in frequency. ^{18}F-FDG PET/CT of patient 13 showed metaphyseal lytic bone destruction, periosteal bone reaction, cortical permeation and soft tissue extension accompanied by abnormally increased glucose metabolism (with early phase SUV_{max} of 13.6 and lag phase SUV_{max} of 16.5). Different from osteosarcoma, there was no sign of mineral deposits or of bone production by the tumor (Supplementary Figure 3).

Differential diagnosis

Malignantly transformed FD needs to be differentiated from adamantinoma (AD). The latter

are low-grade malignant tumors that can occur over a wide age range, but the majority (75%) occur in the mature skeleton within the second and third decades. AD has an exquisite predilection for the tibial diaphyseal cortex; however, the majority (67-88%) show complete involvement of the medullary cavity [17]. Most AD lesions have prominent reactive sclerosis accompanied by moth-eaten or ill-defined margins [18]. Extra-osseous spread and soft-tissue involvement have been reported in approximately 15% of AD [19]. Although not specific, MRI is useful in assessing the extent of the tumor, cortical disruption, and intramedullary extension. In addition, MRI can help delineate multifocal disease and guide preoperative planning [20]. Unlike osteofibrous dysplasia-like adamantinoma (OFD/LA) and AD, FD primarily involves the medullary cavity. Cortical involvement and endosteal scalloping in FD are usually due to the pressure effects of the medullary lesion. Although the definitive diagnosis rests with the pathologist, it is important to stress that FD may be associated with dedifferentiated AD [21].

Focal uptake of ^{99m}Tc-MDP in the context of FD may be similar to that of nonossifying fibroma or a fibrocortical defect (**Figure 1**). The latter has a characteristic appearance on a radiograph of a cortically based lytic lesion, with a thin sclerotic margin, and can show mild uptake on bone scan with more intense uptake during the healing sclerotic phase due to osteoblastic activity. Fusion images of SPECT/CT may help the differential diagnosis under this condition. Osteofibrous dysplasia, which usually occurs in the first two decades of life and affects the tibia and fibula, is a fibro-osseous lesion with many pathologic features similar to that of fibrous dysplasia. Notably, osteofibrous dysplasia characteristically and distinctively involves the cortex as multiple lytic lesions. As we reported previously, most of the involved sites of FD are the extremities and ribs, and the corresponding hot spots usually appear in a bar shape and involve the whole bones. Concerning metastatic bone tumors, hot spots on bone scans and/or ^{99m}Tc-MDP SPECT/CT usually emerge as multiple bone lesions [22]. Some previous studies have demonstrated that ^{18}F-FDG-PET did not play a role in the assessment of FD because FD generally did not uptake ^{18}F-FDG; consequently, these reports implied that the lack of ^{18}F-FDG uptake in FD enabled the identification of glucose-avid bone metastases and osseous lymphoma with FD [23, 24]. By contrast, Stegger et al. reported that benign FD could show elevated uptake of ^{18}F-FDG as well [25]. Here, our study clearly demonstrated that malignantly changed FD, rather than FD, showed markedly increased ^{18}F-FDG uptake (#2, #5, #6, #13, #15). Furthermore, attention should be paid to traumatic history because posttraumatic reactive bony neoformations of the skull can mimic osteosarcoma affecting the craniofacial bones [26].

Treatment and follow-up

For most incidentally discovered asymptomatic FD, no treatment is warranted. Surgery is considered in patients with progressive symptoms or when the disease threatens important anatomical structures [27]. Historically, FD undergoing malignant transformation is treated with extensive amputation. However, due to surgical advances and improved imaging modalities, limb salvage is now considered the standard of care. All of our patients underwent at least one surgery after being diagnosed with FD. Of the 9 patients who received a ^{99m}Tc-MDP bone scan and/or ^{18}F-FDG PET/CT scanning, 5 patients received (#3, #5, #6, #13, #15) a conservative surgery strategy rather than a traditional extensive amputation. Additionally, 9 of the 19 patients received chemotherapy; however, to date, none of the patients have responded substantially. These patients are still under follow-up; therefore, we currently cannot calculate the survival rate of this specific cohort and overall response rate to chemotherapy.

Therapy with bisphosphonates has been suggested to cause pain relief and to have a healing effect on bone lesions. One of our patients received zoledronic acid treatment but showed little efficacy (#11). While some studies demonstrated the efficacy of pamidronate, alendronate, and zoledronic acid in filling in osteolytic lesions and decreasing the rate of bone resorption [28-32], other studies have not shown such effects [33-35]. By far, no randomized controlled clinical trial has been completed thus far. The results from published studies are therefore limited by the lack of a control group. Of note, for patients who have a clear decrease in bone pain following the above-mentioned

treatment, bone scintigraphy is useful in assessing a therapeutic response [33].

Discussion

In addition to the most commonly used X-ray, CT, MRI and bone scintigraphy have been used as corollary imaging modalities in the assessment of FD. Computed tomography demonstrates detailed anatomic information and can exclude a malignant process in certain complex areas such as the spine, pelvis, and skull. FD is typically hypointense or isointense on T1 WI and heterogeneously hyperintense on T2 WI (in relation to skeletal muscle). A surrounding hypointense T1 and T2 rim is often present if there is a sclerotic rind seen on radiographs. Increased uptake on delayed bone scintigraphy is sensitive for the early detection of fibrous dysplasia and for assessing the extent of polyostotic FD, but it is not specific [36]. Therefore, the combination of scintigraphic and radiographic images is complementary in assessing the extent and therapeutic response of disease [22]. Indeed, nearly all of the included patients except one (#8) received systemic medical imaging examinations (**Table 1**). Previously, the role of ^{18}F-FDG PET/CT in the management of FD was controversial. While some studies demonstrated FD lesions as ^{18}F-FDG avid [25], others reported negative abnormal ^{18}F-FDG uptake in patients with FD [23, 24]. There are several potential factors explaining the phenomenon that FD can appear with or without increased ^{18}F-FDG uptakes, such as changes in endocrine function, gender or chemotherapy. Chemotherapy, especially granulocyte colony-stimulating factor (G-CSF), may induce diffuse ^{18}F-FDG uptake in the bone marrow [37]. However, increased focal ^{18}F-FDG concentration on ^{18}F-FDG PET/CT images in the current study, as depicted in **Figures 3**, **4**, Supplementary Figures 2 and 3, was caused by focal malignant transformation of FD rather than other reasons. Although the radiographic appearances of primary osteosarcoma are typical and suggestive of a specific diagnosis, the patterns of secondary osteosarcoma transformed from FD may be delusive. Thus, we highlight that additional imaging modalities, including ^{99m}Tc-MDP bone scan and ^{18}F-FDG PET/CT scanning, can provide vital information for preoperative staging, guiding biopsy and planning surgical management for this specific cohort.

In mono-FD, the zygomatic-maxillary complex is reported to be the region most commonly involved. In the less prevalent poly-FD and MAS, the craniofacial region is involved in 90% of the cases, and the anterior cranial base is involved in over 95% of cases [38]. Consequently, symptoms like facial deformity and asymmetry, vision changes, hearing impairment, nasal congestion and/or obstruction, pain, paresthesia, and malocclusion occur inevitably but vary in different individuals. In some patients, FD is associated with other pathological lesions such as aneurysmal bone cysts (ABCs) or mucoceles [39-41] or, more rarely, with malignant transformation, representing less than 2% of all FD cases [2]. Malignant changes to osteosarcoma [42, 43], fibrosarcoma, chondrosarcoma, and malignant fibrohistiocytoma have been reported previously [44]. Consistently, we confirmed these previous observations as osteosarcoma, the major component of malignantly transformed FD in the cohort reported here. In addition, Ruggieri et al. reported that approximately 50% of malignantly transformed lesions were associated with radiation therapy [2]. However, in our case series, no one had a radiation history, demonstrating that malignancies arise de novo as well. Moreover, the vast majority of secondary osteosarcomas are associated with Paget disease or previous irradiation rather than FD. While the frequency of malignant transformation to osteosarcoma in Paget disease was believed to be approximately 1% [45], radiation-induced osteosarcoma represents 3-5% of all osteosarcomas and 50-60% of all radiation-induced sarcomas [46]. Therefore, comprehensive understanding of the imaging characteristics of bone tumors and exhaustive collection of medical history are of critical importance to make the proper diagnosis and differential diagnosis.

Conclusion

In summary, ^{99m}Tc-MDP SPECT/CT and ^{18}F-FDG PET/CT scanning can play a significant role not only in detecting canceration of fibrous dysplasia but also in optimizing management strategies for patients with malignantly transformed fibrous dysplasia.

Acknowledgements

This work was sponsored by Ph.D. Innovation Fund of Shanghai Jiao Tong University School of Medicine to Wei-Jun Wei (No. BXJ201736).

Disclosure of conflict of interest

None.

Address correspondence to: Quan-Yong Luo, Department of Nuclear Medicine, Shanghai Jiao Tong University Affiliated Sixth People's Hospital, 600# Yishan Road, 200233, Shanghai, China. E-mail: lqyn@sh163.net

References

[1] Harris WH, Dudley HR Jr and Barry RJ. The natural history of fibrous dysplasia. An orthopaedic, pathological, and roentgenographic study. J Bone Joint Surg Am 1962; 44-A: 207-233.

[2] Ruggieri P, Sim FH, Bond JR and Unni KK. Malignancies in fibrous dysplasia. Cancer 1994; 73: 1411-1424.

[3] Shen CT, Wei WJ, Qiu ZL, Song HJ and Luo QY. Value of post-therapeutic ^{131}I scintigraphy in stimulated serum thyroglobulin-negative patients with metastatic differentiated thyroid carcinoma. Endocrine 2016; 51: 283-290.

[4] Qiu ZL, Xu YH, Song HJ and Luo QY. Localization and identification of parapharyngeal metastases from differentiated thyroid carcinoma by ^{131}I-SPECT/CT. Head Neck 2011; 33: 171-177.

[5] Kransdorf MJ, Moser RP Jr and Gilkey FW. Fibrous dysplasia. Radiographics 1990; 10: 519-537.

[6] DiCaprio MR and Enneking WF. Fibrous dysplasia. Pathophysiology, evaluation, and treatment. J Bone Joint Surg Am 2005; 87: 1848-1864.

[7] Berrebi O, Steiner C, Keller A, Rougemont AL and Ratib O. F-18 fluorodeoxyglucose (FDG) PET in the diagnosis of malignant transformation of fibrous dysplasia in the pelvic bones. Clin Nucl Med 2008; 33: 469-471.

[8] AM Davies MS, SL J James. Imaging of Bone Tumors and Tumor-Like Lesions Berlin Heidelberg: Springer; 2009.

[9] Tateishi U, Yamaguchi U, Seki K, Terauchi T, Arai Y and Kim EE. Bone and soft-tissue sarcoma: preoperative staging with fluorine 18 fluorodeoxyglucose PET/CT and conventional imaging. Radiology 2007; 245: 839-847.

[10] Agrawal K, Bhattacharya A, Harisankar CN, Abrar ML, Mittal BR, Tripathy SK and Sen RK. ^{18}F-Fluoride and ^{18}F-fluorodeoxyglucose PET/CT in myositis ossificans of the forearm. Eur J Nucl Med Mol Imaging 2011; 38: 1956.

[11] Nishio J, Nabeshima K, Iwasaki H and Naito M. Non-traumatic myositis ossificans mimicking a malignant neoplasm in an 83-year-old woman: a case report. J Med Case Rep 2010; 4: 270.

[12] Spinelli MS, Perisano C, Della Rocca C, Hardes J, Barone C, Fabbriciani C and Maccauro G. A case of parosteal osteosarcoma with a rare complication of myositis ossificans. World J Surg Oncol 2012; 10: 260.

[13] Tang C, Chan M, Fok M and Fung B. Current management of hand enchondroma: a review. Hand Surg 2015; 20: 191-195.

[14] Ramirez-Bollas J, Padilla-Rosciano A, Romero YHA, Lavin-Lozano AJ, Medina-Castro JM, Dubon-Garcia E and Turcios-Cadenas ER. [Maffucci's syndrome. Case reports and literature review]. Cir Cir 2005; 73: 217-221.

[15] Ngai C, Ding DY and Rapp TB. Maffucci Syndrome. An interesting case and a review of the literature. Bull Hosp Jt Dis (2013) 2015; 73: 282-285.

[16] Pansuriya TC, Kroon HM and Bovee JV. Enchondromatosis: insights on the different subtypes. Int J Clin Exp Pathol 2010; 3: 557-569.

[17] Bethapudi S, Ritchie DA, Macduff E and Straiton J. Imaging in osteofibrous dysplasia, osteofibrous dysplasia-like adamantinoma, and classic adamantinoma. Clin Radiol 2014; 69: 200-208.

[18] Keeney GL, Unni KK, Beabout JW and Pritchard DJ. Adamantinoma of long bones. A clinicopathologic study of 85 cases. Cancer 1989; 64: 730-737.

[19] Kahn LB. Adamantinoma, osteofibrous dysplasia and differentiated adamantinoma. Skeletal Radiol 2003; 32: 245-258.

[20] Holden DM, Joyce MJ and Sundaram M. Adamantinoma. Orthopedics 2014; 37: 362, 420-362.

[21] Nouri H, Jaafoura H, Bouaziz M, Ouertatani M, Abid L, Meherzi MH, Ladeb MF and Mestiri M. Dedifferentiated adamantinoma associated with fibrous dysplasia. Orthop Traumatol Surg Res 2011; 97: 770-775.

[22] Zhibin Y, Quanyong L, Libo C, Jun Z, Hankui L, Jifang Z and Ruisen Z. The role of radionuclide bone scintigraphy in fibrous dysplasia of bone. Clin Nucl Med 2004; 29: 177-180.

[23] Toba M, Hayashida K, Imakita S, Fukuchi K, Kume N, Shimotsu Y, Cho I, Ishida Y, Takamiya M and Kumita S. Increased bone mineral turnover without increased glucose utilization in sclerotic and hyperplastic change in fibrous dysplasia. Ann Nucl Med 1998; 12: 153-155.

[24] Shigesawa T, Sugawara Y, Shinohara I, Fujii T, Mochizuki T and Morishige I. Bone metastasis detected by FDG PET in a patient with breast cancer and fibrous dysplasia. Clin Nucl Med 2005; 30: 571-573.

[25] Stegger L, Juergens KU, Kliesch S, Wormanns D and Weckesser M. Unexpected finding of elevated glucose uptake in fibrous dysplasia mimicking malignancy: contradicting metabo-

lism and morphology in combined PET/CT. Eur Radiol 2007; 17: 1784-1786.
[26] Pfeiffer J, Kayser G, Boedeker CC and Ridder GJ. Posttraumatic reactive fibrous bone neoformation of the anterior skull base mimicking osteosarcoma. Skull Base 2008; 18: 345-351.
[27] Feller L, Wood NH, Khammissa RA, Lemmer J and Raubenheimer EJ. The nature of fibrous dysplasia. Head Face Med 2009; 5: 22.
[28] Chapurlat RD, Hugueny P, Delmas PD and Meunier PJ. Treatment of fibrous dysplasia of bone with intravenous pamidronate: long-term effectiveness and evaluation of predictors of response to treatment. Bone 2004; 35: 235-242.
[29] Parisi MS, Oliveri B and Mautalen CA. Effect of intravenous pamidronate on bone markers and local bone mineral density in fibrous dysplasia. Bone 2003; 33: 582-588.
[30] Lane JM, Khan SN, O'Connor WJ, Nydick M, Hommen JP, Schneider R, Tomin E, Brand J and Curtin J. Bisphosphonate therapy in fibrous dysplasia. Clin Orthop Relat Res 2001; 6-12.
[31] Isaia GC, Lala R, Defilippi C, Matarazzo P, Andreo M, Roggia C, Priolo G and de Sanctis C. Bone turnover in children and adolescents with McCune-Albright syndrome treated with pamidronate for bone fibrous dysplasia. Calcif Tissue Int 2002; 71: 121-128.
[32] Lala R, Matarazzo P, Bertelloni S, Buzi F, Rigon F and de Sanctis C. Pamidronate treatment of bone fibrous dysplasia in nine children with McCune-Albright syndrome. Acta Paediatr 2000; 89: 188-193.
[33] Thomsen MD and Rejnmark L. Clinical and radiological observations in a case series of 26 patients with fibrous dysplasia. Calcif Tissue Int 2014; 94: 384-395.
[34] Plotkin H, Rauch F, Zeitlin L, Munns C, Travers R and Glorieux FH. Effect of pamidronate treatment in children with polyostotic fibrous dysplasia of bone. J Clin Endocrinol Metab 2003; 88: 4569-4575.
[35] Chan B and Zacharin M. Pamidronate treatment of polyostotic fibrous dysplasia: failure to prevent expansion of dysplastic lesions during childhood. J Pediatr Endocrinol Metab 2006; 19: 75-80.
[36] Leet AI, Magur E, Lee JS, Wientroub S, Robey PG and Collins MT. Fibrous dysplasia in the spine: prevalence of lesions and association with scoliosis. J Bone Joint Surg Am 2004; 86-A: 531-537.
[37] Sugawara Y, Fisher SJ, Zasadny KR, Kison PV, Baker LH and Wahl RL. Preclinical and clinical studies of bone marrow uptake of fluorine-1-fluorodeoxyglucose with or without granulocyte colony-stimulating factor during chemotherapy. J Clin Oncol 1998; 16: 173-180.
[38] Lee JS, FitzGibbon EJ, Chen YR, Kim HJ, Lustig LR, Akintoye SO, Collins MT and Kaban LB. Clinical guidelines for the management of craniofacial fibrous dysplasia. Orphanet J Rare Dis 2012; 7 Suppl 1: S2.
[39] Lee JS, FitzGibbon E, Butman JA, Dufresne CR, Kushner H, Wientroub S, Robey PG and Collins MT. Normal vision despite narrowing of the optic canal in fibrous dysplasia. N Engl J Med 2002; 347: 1670-1676.
[40] Michael CB, Lee AG, Patrinely JR, Stal S and Blacklock JB. Visual loss associated with fibrous dysplasia of the anterior skull base. Case report and review of the literature. J Neurosurg 2000; 92: 350-354.
[41] Diah E, Morris DE, Lo LJ and Chen YR. Cyst degeneration in craniofacial fibrous dysplasia: clinical presentation and management. J Neurosurg 2007; 107: 504-508.
[42] Sadeghi SM and Hosseini SN. Spontaneous conversion of fibrous dysplasia into osteosarcoma. J Craniofac Surg 2011; 22: 959-961.
[43] Reis C, Genden EM, Bederson JB and Som PM. A rare spontaneous osteosarcoma of the calvarium in a patient with long-standing fibrous dysplasia: CT and MR findings. Br J Radiol 2008; 81: e31-34.
[44] Tsai EC, Santoreneos S and Rutka JT. Tumors of the skull base in children: review of tumor types and management strategies. Neurosurg Focus 2002; 12: e1.
[45] Wick MR, Siegal GP, Unni KK, McLeod RA and Greditzer HG 3rd. Sarcomas of bone complicating osteitis deformans (Paget's disease): fifty years' experience. Am J Surg Pathol 1981; 5: 47-59.
[46] Fletcher CD, Unni KK and Mertens F. Pathology and genetics of tumours of soft tissue and bone. IARC; 2002.

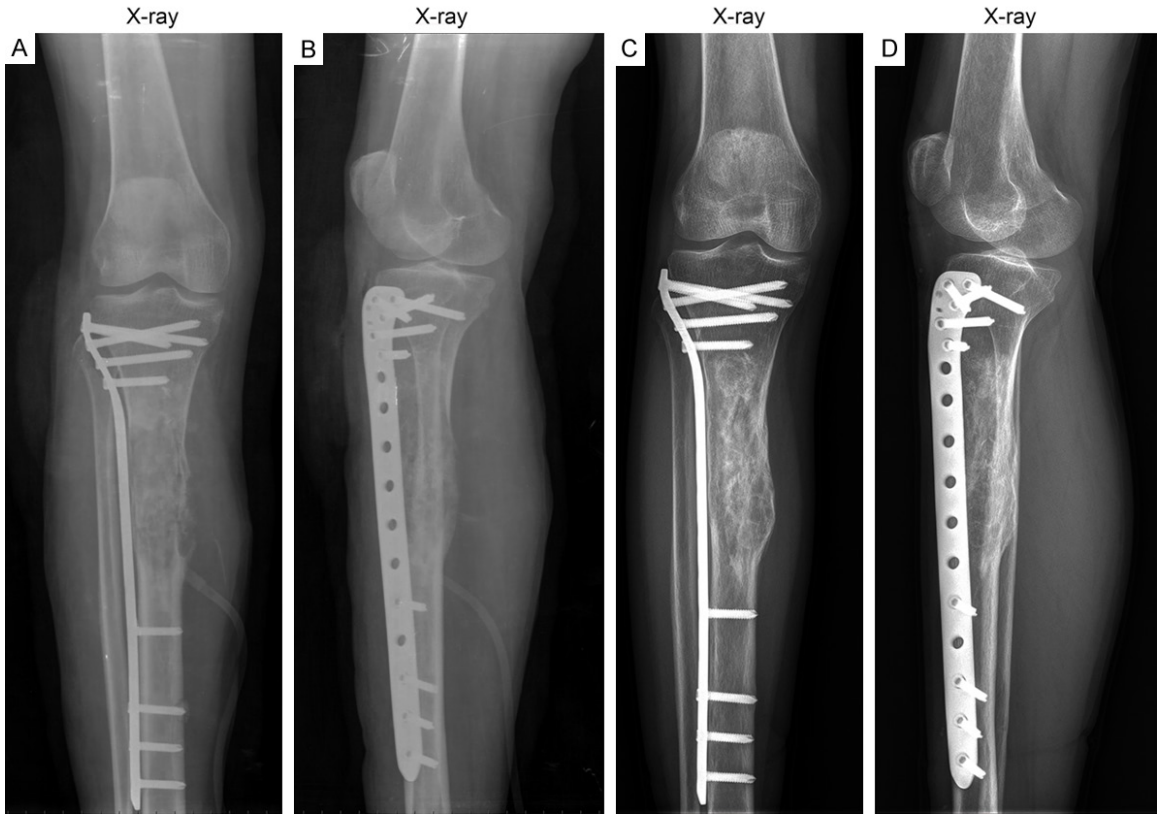

Supplementary Figure 1. Malignant transformation of fibrous dysplasia to osteosarcoma in a 45-year-old female presenting with swelling and pain (patient 3). A, B: Anteroposterior and lateral radiographs performed after initial surgery. C, D: Anteroposterior and lateral radiographs performed four years later at follow-up.

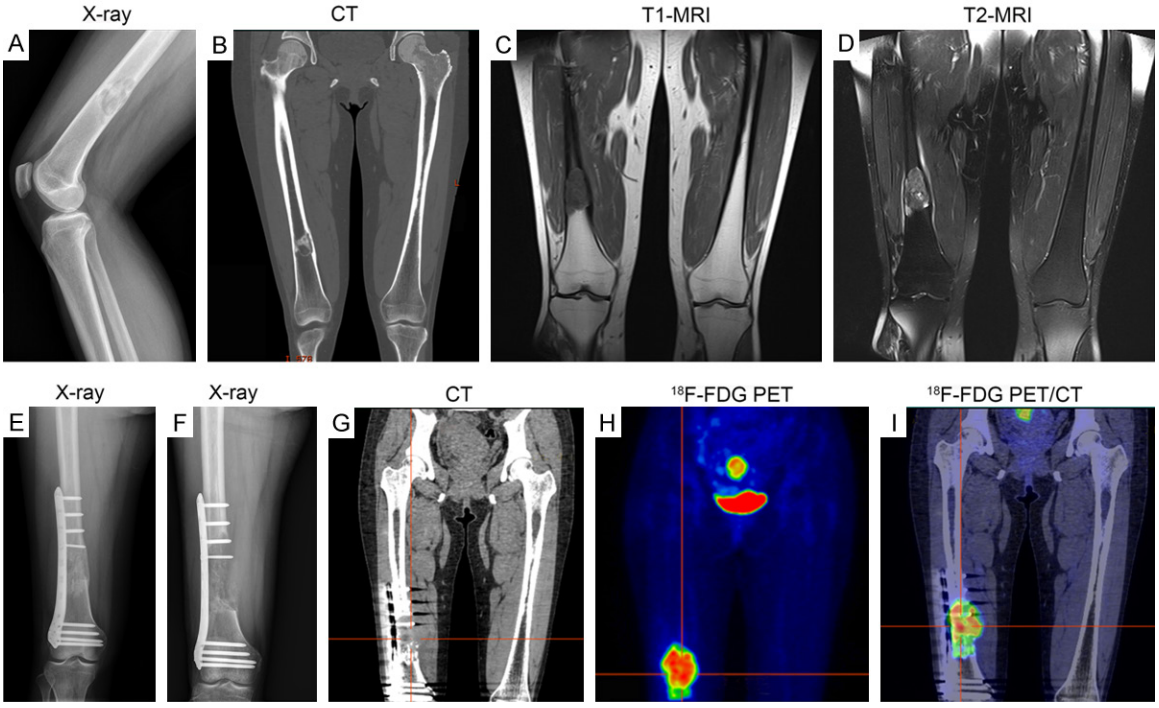

Supplementary Figure 2. A 46-year-old female patient with malignantly transformed FD. A: The lateral radiograph showed an expansile lytic lesion involving the right posterior femur (10/2013). B: Note the ground-glass appearance

with internal septa on the coronal CT image. C: The coronal T1-weighted image showed that the lesion was hypointense and infiltrated into the adjacent cortical bone. D: Coronal fat-suppressed MRI image confirmed the cortical involvement and surrounding dropsy. E: Anteroposterior radiograph taken after initial curettage and fixation surgery. F: Anteroposterior radiograph taken one year after initial surgery found disruption of the diseased area (10/2014). G-I: Subsequent ^{18}F-FDG PET/CT scanning of the patient demonstrated focal intense ^{18}F-FDG uptake accompanied by bone destruction without bone metastasis and distant metastasis. The patient then underwent tumorous end removal and artificial limb replacement. To date, the patient lives quite well without any disease recurrence or remnants.

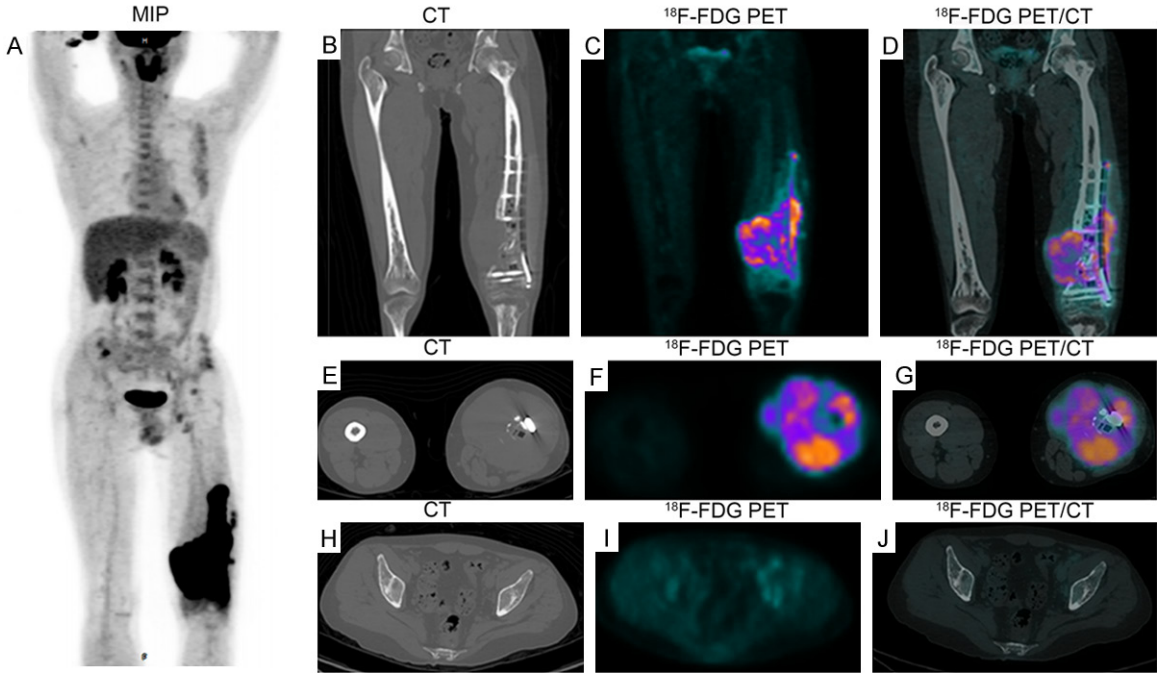

Supplementary Figure 3. Concomitant malignant transformation of fibrous dysplasia to osteosarcoma and fibrosarcoma in a 35-year-old man presenting with pathological fracture (patient 13). A: ^{18}F-FDG PET/CT scanning after initial fixation surgery (11/2011), MIP image showed multiple abnormal radiotracer uptakes in the cervix, armpit, groin and lower left femur. B-G: Coronal and axial ^{18}F-FDG PET/CT fusion images of the bilateral femurs demonstrated disunion of the fractured femur and involvement of adjacent soft tissue accompanied by increased ^{18}F-FDG uptake. H-J: ^{18}F-FDG PET/CT fusion images of the pelvis showed dense lesions in the bilateral iliac bones without radiotracer uptake, possibly representing normal fibrous dysplasia or other benign bone tumors.